

ATX-LPA axis facilitates estrogen-induced endometrial cancer cell proliferation via MAPK/ERK signaling pathway

GUO ZHANG^{*}, YUAN CHENG^{*}, QI ZHANG, XIAOPING LI, JINGWEI ZHOU, JIANLIU WANG and LIHUI WEI

Department of Gynecology and Obstetrics, Peking University People's Hospital, Beijing 100044, P.R. China

Received June 7, 2017; Accepted November 10, 2017

DOI: 10.3892/mmr.2018.8392

Abstract. Autotaxin (ATX) is a key enzyme that converts lysophosphatidylcholine to lysophosphatidic acid (LPA). ATX is a crucial factor that facilitates cancer progression; however, the effect of ATX on endometrial cancer has not been explored. The aim of the present study was to investigate the role of ATX in the progression of endometrial cancer. The immunohistochemical results revealed higher protein expression levels of ATX and LPA receptors (LPA 1, 2 and 3) in human endometrial cancer tissue than in non-carcinoma tissue. In addition, reverse transcription-quantitative polymerase chain reaction and western blotting analysis demonstrated that ATX and LPA receptor mRNA and protein expression was greater in Ishikawa cells, which are positive for estrogen receptor (ER), than in Hec-1A cells that exhibit low ER expression. Short interfering RNA knockdown of ATX in Ishikawa cells led to decreased cell proliferation and cell colony number, as determined by Cell Counting kit-8 and colony formation assays. Estrogen stimulated ATX mRNA expression. Inhibition of ATX decreased estrogen and LPA-induced cell proliferation. High LPA levels markedly elevated the phosphorylation levels of extracellular signal-regulated kinase (ERK). ATX down-regulation moderately decreased estrogen- and LPA-induced phosphorylation of ERK. In addition, the ERK inhibitor, PD98059, reduced cell proliferation with estrogen, ATX and LPA treatment. The present study suggested that the ATX-LPA axis may facilitate estrogen-induced cell proliferation in endometrial cancer via the mitogen-activated protein kinase/ERK signaling pathway. The present study may provide ideas and an experimental basis for clinicians to identify new molecular targeted drugs for the treatment of endometrial cancer.

Introduction

Endometrial carcinoma is one of the three malignant tumors of the female genital tract, accounting for 20 to 30% of the total number of female genital-tract malignant tumors (1). In 2015, 54,870 new cases of endometrial carcinoma were diagnosed worldwide, and the number of mortalities was ~10,170 (2). Early endometrial cancer has a good prognosis; however, ~7% of cases recur and the 3-year survival rate is relatively poor (3). Therefore, the underlying molecular mechanism of endometrial cancer must be studied to prevent further cancer development and to improve prognosis.

A previous study has suggested that the underlying mechanisms of occurrence of endometrial cancer include an estrogen and progesterone imbalance and tumor microenvironment factors (4). Autotaxin (ATX) is a key factor that regulates the tumor microenvironment. It is a primary secreted enzyme with lysophospholipase D activity to catalyze lysophosphatidylcholine (LPC) to lysophosphatidic acid (LPA). LPA, a simple-structured glycerophospholipid, is an intercellular lipid signaling molecule. LPA may bind to LPA receptors (LPA1-7), which are G-protein coupled receptors, enabling LPA to exert multiple biological functions. ATX has diverse roles in various different types of cancers via the LPA and LPA receptors; these two represent the ATX-LPA axis (5).

ATX promotes tumor cell proliferation, invasion, metastasis and angiogenesis, which are closely associated with LPA. In breast cancer, the ATX-LPA axis promotes the proliferation of mammary epithelial cell lines (6). The effect of LPC on cell migration was observed to be reduced by inhibiting the secretion of ATX in human breast cancer and melanoma cells. LPC promotes cell migration mediated by LPA catalyzed by ATX (7). A positive feedback loop was identified between ATX and vascular endothelial growth factor (VEGF) in ovarian cancer cell lines. Exogenous VEGF may promote the expression and secretion of ATX, and increase extracellular LPA production. Accordingly, LPA induced VEGF receptor expression may regulate the cellular response to VEGF (8). A previous study demonstrated that LPA2 promoted the invasion of Hec-1A cells in endometrial cancer. LPA2 increased the secretion of matrix metalloproteinase 7, which suggested that LPA2 is an important factor in accelerating the progression of endometrial carcinoma (9).

However, it appears that the role of ATX in endometrial cancer has not yet been explored. The present study

Correspondence to: Professor Jianliu Wang, Department of Gynecology and Obstetrics, Peking University People's Hospital, 11 Xizhimen South Street, Beijing 100044, P.R. China
E-mail: wangjianliu@pkuph.edu.cn

^{*}Contributed equally

Key words: endometrial cancer, autotaxin, lysophosphatidic acid, proliferation, estrogen

investigated the effect of the ATX-LPA axis on endometrial cancer cell proliferation. As the majority of endometrial cancers are estrogen-dependent, the present study aimed to identify the interaction between the ATX-LPA axis and estrogen in endometrial cancer progression. Finally, this study preliminarily clarified the underlying molecular mechanism of the ATX-LPA axis in endometrial cancer.

Materials and methods

Reagents and antibodies. Recombinant human ATX (also known as Ectonucleotide Pyrophosphatase/Phosphodiesterase-2) was purchased from R&D Systems, Inc., Minneapolis, MN, USA. 1-Oleoyl lysophosphatidic acid sodium salt was from Tocris Bioscience (Bristol, UK). 17- β estradiol (estrogen) was from Sigma-Aldrich; Merck KGaA (Darmstadt, Germany). PD98059 [the phosphorylated extracellular signal-regulated kinase (p-ERK) inhibitor] was from Invitrogen (Thermo Fisher Scientific, Inc., Waltham, MA, USA). ATX antibody for western blotting was from Abcam (Cambridge, UK; ab77104) and for immunohistochemistry from Santa Cruz Biotechnology (Texas, USA; sc-374222). Antibodies against LPA receptors (LPA1, LPA2, LPA3) were from Abcam (ab166903, ab38322 and ab219267, respectively). Total/phosphorylated extracellular signal-regulated kinases (t/p-ERK) were from Cell Signaling Technology, Inc. Danvers, MA, USA (4695s and 4370s). Antibodies against GAPDH were from Santa Cruz Biotechnology (sc-51907). Crystal violet staining solution was from Tiangen Biotech Co., Ltd. (Beijing, China). Cell Counting kit (CCK)-8 was from Beyotime Institute of Biotechnology, Haimen, China (C0037). Transwell culture plates were from Corning Incorporated (Corning, NY, USA). Lipofectamine 2000TM transfection reagent was from Invitrogen, Thermo Fisher Scientific, Inc.

Cell culture, siRNA and transfection. Ishikawa and Hec-1A cells are endometrial adenocarcinoma cell lines. Ishikawa cells were kindly provided by Dr Jonathan Braun (David Geffen School of Medicine, University of California, CA, USA) and kept and subcultivated in our laboratory; they are positive for estrogen receptor (ER). Ishikawa cells were cultured in F12-Dulbecco's modified Eagle's medium (M&C Gene Technology, Ltd., Beijing, China) supplemented with 10% fetal bovine serum (FBS; HyClone; GE Healthcare, Chicago, IL, USA) at 37°C with 5% CO₂ in a humidified atmosphere. The Hec-1A cell line was from American Type Culture Collection (ATCC; Manassas, VA, USA). Hec-1A cells with low ER expression were cultured in McCoy's 5A medium (M&C Gene Technology, Ltd.), as recommended by ATCC. Non-specific short interfering (si)RNA (si-NC) and two siRNA sequences specific to ATX were synthesized by Shanghai GenePharma Co., Ltd. (Shanghai, China; negative control: Sense: 5'-UUC UCCGAACGUGUCACGUTT-3', Antisense: 5'-ACGUGA CAGUUCGGAGAATT-3'; ATX-siRNA1: Sense: 5'-AUC GACAAA AUUGUGGGGCTT-3', Antisense: 5'-GCCCCA CAUUUUGUCGAUTT-3'; ATX-siRNA2: Sense: 5'-CGU CAUCUUUGUCGGAGACTT-3', Antisense: 5'-GUCUCC GACAAAGAUGACGTT-3'). Ishikawa and Hec-1A cells were grown until 60-70% confluent, and transfected with ATX siRNAs or siRNA-NC as a negative control at 100 nm by using

Lipofectamine[®] 2000 (Invitrogen; Thermo Fisher Scientific, Inc.). The serum-free medium (DMEM-F12 without FBS) with transfected siRNA was replaced with culture medium (DMEM-F12 with 10% FBS) following 6 h incubation. The transfected cells continued to be cultured until 48 h at 37°C in a 5% CO₂ incubator.

Reverse transcription-quantitative polymerase chain reaction (RT-qPCR). Total RNA was isolated from the transfected cells with ATX siRNAs or siRNA-NC by using TRIzol (Thermo Fisher Scientific, Inc.) according to the manufacturer's protocol. Reverse transcription and cDNA synthesis involved the use of oligo-dT primers with 2 μ g total RNA and Superscript III reverse transcriptase according to the First Strand cDNA Synthesis kit (cat no. KR108; Tiangen Biotech Co., Ltd.). PCR involved use of 5% total cDNA and was amplified with primers (ATX forward primer: 5'-CTTTCGGCCCTGAGGAGA GTA-3', ATX reverse primer: AGCAACTGGTCTTTCCTG TCT; LPA1 forward primer: 5'-AATCGGGATACCATGATG AGTCTT-3', LPA1 reverse primer: 5'-CCAGGAGTCCAG CAGATGATAAA-3'; LPA2 forward primer: 5'-CGCTCA GCCTGGTCAAGACT-3', LPA2 reverse primer: 5'-TTGCAG GACTCACAGCCTAAAC-3'; LPA3 forward primer: 5'-AGG ACACCCATGAAGCTAATGAA-3', LPA3 reverse primer: 5'-GCCGTCGAGGAGCAGAAC-3'; GAPDH forward primer: CCTCCGGGAAACTGTGGCGTGATGG; GAPDH reverse primer: AGACGGCAGGTCAGGTCCACCACTG), using the FastFire qPCR PreMix (SYBR Green; cat no. FP207; Tiangen Biotech Co., Ltd.) with the thermocycling conditions of 95°C for 5 sec, 56°C for 10 sec and 72°C for 15 sec for 40 cycles with the iCyclerIQ real-time PCR detection system (Bio-Rad Laboratories, Inc., Hercules, CA, USA). Melting curve analysis was performed for each sample to ensure that a single product was produced in each reaction. The 2^{- $\Delta\Delta$ C_q} method was used for quantification (10).

Immunohistochemistry. The tissues of 10 endometrial carcinoma patients were obtained previously from the Pathology Department of Peking University People's Hospital (Beijing, China). The pathological sections were already processed and paraffin embedded routinely following surgery.

The present study was approved by the ethics committee of Peking University People's Hospital (approval no. 2016PHB054-01). Slides of cancer samples continuous with surrounding endometrial tissue were determined by a pathologist in Pathology Department of Peking University People's Hospital. First, slides were dewaxed in xylene twice. After that, different concentrations of alcohol (95, 85 and 75%) were used to continue dewaxing and slides were then placed in water. Subsequently, peroxide enzyme was removed by adding 30% H₂O₂ to the slides, which were then washed three times with 1XPBS. Sections were then incubated with sealing fluid (ZLI-9022; OriGene Technologies, Inc., Beijing, China) for 30 mins, and then the following primary antibodies: Mouse anti-ATX (sc-374222; Santa Cruz Biotechnology), rabbit anti-LPA1, 2 and 3 (ab166903, ab38322 and ab219267; Abcam) (dilution 1:400) and 1x PBS (negative control) at 4°C for 12 h. Sections were then probed with the mouse and rabbit secondary antibodies (PV-6001 and PV-6002; OriGene Technologies, Inc.) for 1 h at room temperature, followed

by 3,3'-diaminobenzidine color solution (ZLI-9018; OriGene Technologies, Inc.) for 20 sec each section at room temperature. The immunohistochemical results were analyzed using Image-Pro Plus software version 6.0 (Media Cybernetics, Inc., Rockville, MD, USA). From 5 randomly selected fields of each section (x400) images were captured using a light microscope (Eclipse 501; Nikon Corporation, Tokyo, Japan), the mean density (IOD SUM/area) and integrated optical density (IOD) value of positive stained areas were calculated and thence each sample's mean density. ATX, LPA1, LPA2 and LPA3 protein expression of 10 endometrial cancers and 10 non-carcinoma tissues samples were compared by t-test analysis.

Western blot analysis. The cells (2×10^6 from each well in 6-wells plates) were harvested, washed three times with 1XPBS, and lysed in lysis buffer (R0020; Beijing Solarbio Science & Technology Co., Ltd., Beijing, China) for 30 min on ice. The lysates were centrifuged (15 min at $12,000 \times g$, 4°C), and the protein concentration was determined by a bicinchoninic acid protein assay kit (23225; Thermo Fisher Scientific, Inc.). A total of 20-60 μg protein in each sample was separated by 10% SDS-PAGE and transferred onto nitrocellulose filter membranes (Merck KGaA). Membranes for target protein (ATX, LPA1, LPA2, LPA3 and GAPDH) were blocked with 5% skimmed milk for 1 h at room temperature. Membranes for interest protein (T-ERK and P-ERK) were blocked with 5% bovine serum albumin (BSA; B2064-50G; Sigma-Aldrich; Merck KGaA) for 1 h at room temperature. These membranes were separately incubated with primary antibodies ATX (ab77104; 1:1,000; Abcam), LPA1 (ab166903; 1:1,000, Abcam), LPA2 (ab38322; 1:1,000; Abcam), LPA3 (ab219267; 1:1,000; Abcam), T-ERK (4695s; 1:1,000; Cell Signaling Technology, Inc.), P-ERK (4370s; 1:1,000; Cell Signaling Technology, Inc.) and GAPDH (sc-51907; 1:5,000; Santa Cruz Biotechnology), with the 5% skimmed milk or BSA dilutions recommended by the manufacturer, at 4°C overnight. Membranes were then washed using 1XTBST with 0.1% Tween-20 and incubated with 1:3,000 secondary goat anti-rabbit IgG (ZB-2301; OriGene Technologies, Inc.) or goat anti-mouse IgG antibodies (ZB-2305; OriGene Technologies, Inc.). The membrane was incubated with luminol reagent and enhanced chemiluminescence (Lot No. 1614602, EMD Millipore, Billerica, MA, USA) for 30-120 sec at room temperature. The optical density of bands was quantified by using ImageJ software (v2.1.4.7; National Institutes of Health, Bethesda, MD, USA).

CCK8 assay. Ishikawa cells grown until 60-70% confluent were transfected with siRNA-NC or ATX siRNA and cultured for 24 h at 37°C with 5% CO_2 in a humidified atmosphere, then cells were seeded in 96-well culture plates at 2,000 cells per well. The absorbance values of almost immediately adherent cells 4 h after seeding were measured as the control group. Cells were incubated with CCK8 (C0037; 1:100; Beyotime Institute of Biotechnology) for 2 h at 37°C . Absorbance was measured at a wavelength of 450 nm using a microplate reader. Next, cell absorbance values were detected using CCK8 methods at days 1, 2, 3, and 4, respectively. Alternatively, cells were transfected with ATX siRNA and cultured for 24 h at 37°C , then seeded in 96-well culture plates at 2,000 cells per well and treated with 10 nM 17β -estradiol or 40 μM LPA for 48 h at 37°C . Cells

were collected, incubated with CCK8 and the absorbance was measured as described above. In addition, cells were treated with 100 μM PD98059 (the p-ERK inhibitor) for 24 h at 37°C , then seeded in 96-well culture plates at 2,000 cells per well and treated with 10 nM 17β -estradiol or 40 μM LPA/0.5 nM ATX for 48 h at 37°C . Cells were then collected, incubated with CCK8 and the absorbance was measured as described above.

Colony formation assay. Ishikawa cells grown until 60-70% confluent were transfected with siRNA and cultured for 24 h at 37°C , rinsed with PBS twice, then digested with 0.25% trypsin solution for 2 min at 37°C . The neutralization reaction was induced by adding DMEM-F12 with 10% FBS and cells were centrifuged for 5 min at $300 \times g$ at room temperature, liquid-decanted and 1 ml fresh culture medium was added. Cells were dispersed by pipetting repeatedly to create a single-cell suspension with culture medium. Subsequently, cells were counted using a cell counting chamber. A total of 500 cells were added to each well of 6-well culture plates for ~6 days and the medium was replaced every 3 days until cell clones were observed with the naked eye. Cells were washed with PBS twice and fixed in 4% paraformaldehyde for 15 min at room temperature. Cells were then stained with crystal violet for 5 min at room temperature, dried, images captured using an inverted microscope and counted using ImageJ software (version 2.1.4.7; National Institutes of Health).

Statistical analysis. Data are expressed as the mean \pm standard error. All experiments were repeated 3 times. Quantitative results were compared using GraphPad Prism version 5.0 software (GraphPad Software, Inc., La Jolla, CA, USA). A two-tailed Student's paired t-test was used to test for significance between two groups. Multiple groups were compared by a one-way or two-way analysis of variance with Tukey's post-test correction. $P < 0.05$ was considered to indicate a statistically significant difference.

Results

Expression of ATX and LPA1, 2 and 3 in endometrial carcinoma tissues. Pathological sections of normal adjacent tissues and carcinoma tissues were obtained from 10 endometrial adenocarcinoma patients. Following immunohistochemistry, 5 randomly selected fields of stained pathological sections were photographed under a light microscope at x400 magnification. The absorbance value of positive regions was analyzed using the Image-Pro Plus software version 6.0 (Media Cybernetics, Inc.). ATX expression was stronger in endometrial carcinoma than in adjacent non-cancerous tissue (Fig. 1A and C). Also, ATX was expressed in the cytoplasm of cancer cells and stromal cells. LPA1, 2, 3 expression levels were greater in endometrial cancer tissues than in adjacent non-cancerous tissue (Fig. 1B and C).

Differential expression of ATX and LPA1, 2 and 3 in endometrial cancer cells. Ishikawa cells positive for ER and Hec-1A cells with low ER expression exhibited ATX expression (Fig. 2A). However, ATX mRNA expression was higher in Ishikawa cells than in Hec-1A cells (Fig. 2A).

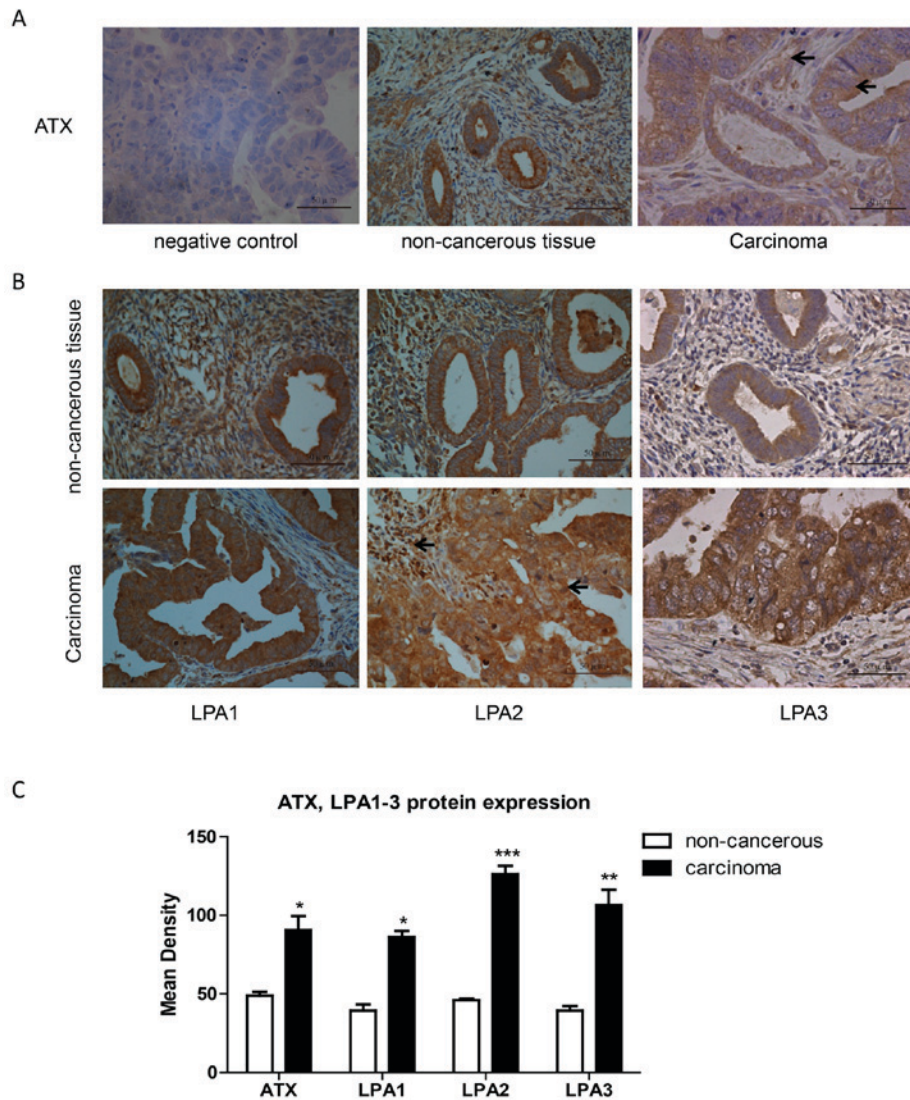


Figure 1. Greater expression of ATX and LPA1, 2 and 3 in 10 endometrial carcinoma tissues than in adjacent non-cancerous tissues. Immunohistochemistry staining of (A) ATX and (B) LPA 1, 2 and 3 protein expression in endometrial carcinoma tissues and adjacent non-cancerous tissue by inverted microscopy. All images of the stained sections were captured at $\times 400$ magnification. Arrows (\rightarrow) show the localization of the staining in cancer cells and stromal cells. (C) Quantification of immunohistochemical staining of 10 endometrial carcinoma tissues and adjacent non-cancerous tissues. * $P < 0.05$, ** $P < 0.01$ and *** $P < 0.001$ vs. adjacent non-cancerous tissues. ATX, autotaxin; LPA, lysophosphatidic acid.

ATX was primarily expressed in the cytoplasm of the cells by immunocytochemistry (Fig. 2B). ATX protein expression was also greater in Ishikawa cells than in Hec-1A cells (Fig. 2C and D). The mRNA expression levels of LPA1, 2 and 3 were detected in both cell types, and LPA2 expression was the greatest (Fig. 2E and F).

siRNA knockdown of ATX inhibits the proliferation of Ishikawa cells. To understand the role of ATX in endometrial adenocarcinoma, 2 siRNA sequences were used to obtain loss of function of ATX in Ishikawa cells. The mRNA and protein expression levels of ATX were significantly decreased following siRNA knockdown of ATX compared with Ishikawa cells transfected with siRNA-NC (Fig. 3A and B). The CCK8 assay revealed that the rate of cell growth was slower in cells transfected with ATX siRNA than in Ishikawa cells transfected with siRNA-NC (Fig. 3C). In addition, Ishikawa cells exhibited lower colony numbers following ATX knockdown (Fig. 3D).

Reduced ATX levels decrease proliferation of Ishikawa cells induced by estrogen and LPA. ATX expression was significantly increased in Ishikawa cells positive for ER. It was then determined whether estrogen induced the expression of ATX by examining the mRNA expression of ATX in Ishikawa cells treated with 17β -estradiol for 24 h. The mRNA expression of ATX was significantly induced by estrogen compared with the control (Fig. 4A). It was subsequently determined whether ATX was involved in estrogen- and LPA-induced cell proliferation. Inhibition of ATX with siRNA decreased the cell proliferation induced by estrogen, LPA or estrogen in combination with LPA (Fig. 4B-D).

ATX-LPA is involved in estrogen-induced cell proliferation via ERK signaling. To confirm the effect of ATX on LPA receptors, Ishikawa cells were transfected with ATX siRNA, and then the mRNA expression levels of LPA1, 2 and 3 were determined. To varying degrees, the expression of LPA 1, 2 and 3 receptors

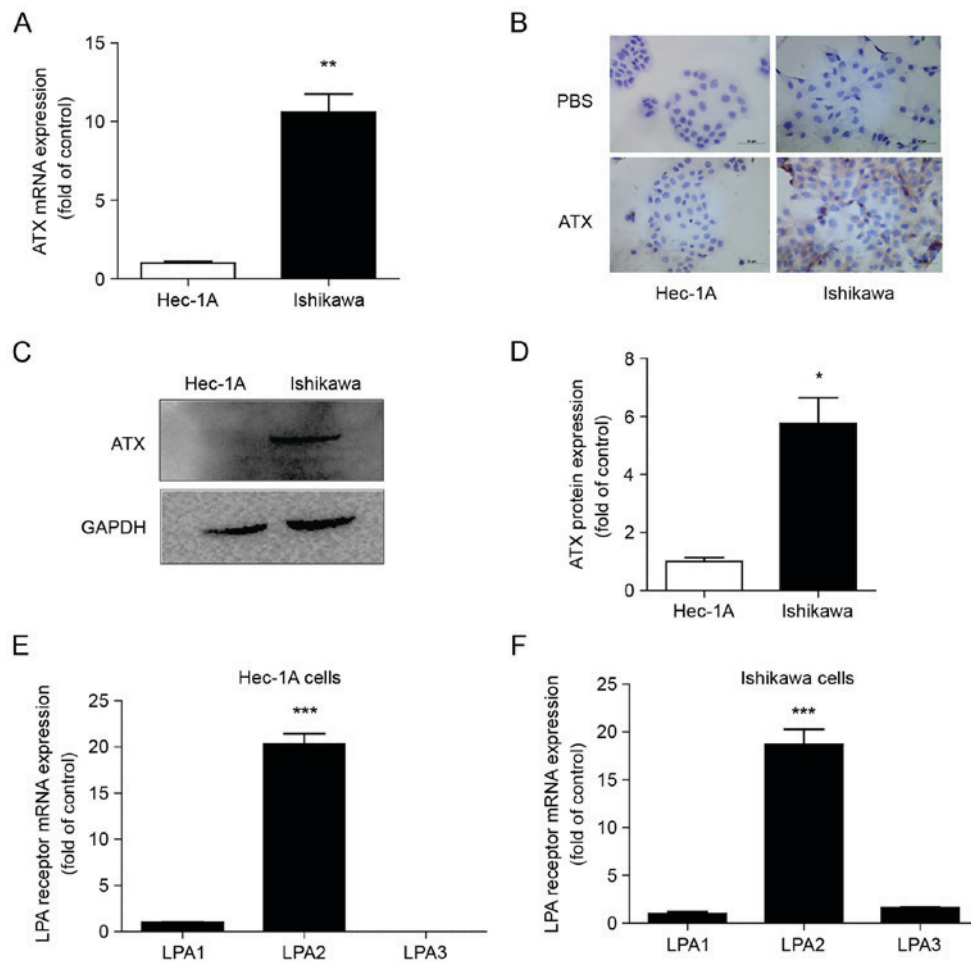


Figure 2. Expression levels of ATX and LPA1, 2 and 3 in two different endometrial cancer cell lines. (A) Reverse transcription-quantitative polymerase chain reaction analysis of ATX mRNA expression levels in Ishikawa and Hec-1A cells. (B) ATX localization by immunocytochemistry and (C and D) protein expression levels by western blot analysis in Hec-1A and Ishikawa cells. * $P < 0.05$ and ** $P < 0.01$ vs. Hec-1A cells. Reverse transcription-quantitative polymerase chain reaction of LPA 1, 2 and 3 mRNA expression levels in (E) Hec-1A cells and (F) Ishikawa cells. *** $P < 0.001$ vs. LPA1. GAPDH was used as an internal reference. Data are shown as the mean \pm standard deviation ($n=3$). ATX, autotaxin; LPA, lysophosphatidic acid.

was reduced following ATX siRNA treatment when compared with the siRNA-NC group, and LPA2 expression was the most significantly reduced (Fig. 5A). Ishikawa cells were subsequently treated with different concentrations of LPA. LPA at 80, 40 and 20 μM significantly increased the phosphorylation of ERK compared with 0 μM (Fig. 5B). p-ERK expression levels were downregulated following siRNA knockdown of ATX compared with the siRNA-NC group (Fig. 5C). Transfection with ATX siRNA reduced LPA or estrogen-induced ERK phosphorylation (Fig. 5D and E). In addition, inhibition of the ERK signaling pathway by PD98059 with estrogen and/or ATX and LPA treatment decreased cell proliferation (Fig. 5F and G).

Discussion

Endometrial adenocarcinoma represents 87 to 90% of all diagnosed endometrial carcinomas. In the present study, ATX and LPA receptors were highly expressed in endometrial adenocarcinoma compared with surrounding non-cancerous endometrial tissue. The expression levels of ATX and LPA receptors were positive in the cytoplasm of endometrial cancer cells. Hence, the ATX-LPA axis may serve an important role in the progression of endometrial adenocarcinoma.

Wasniewski *et al* (11) investigated ATX and LPA receptor expression in 37 endometrial cancers and 10 normal endometrial samples, and demonstrated that ATX and LPA receptors were overexpressed in endometrial carcinoma. High expression of LPA1 and 2 was positively associated with the depth of myoinvasion, International Federation of Gynecology and Obstetrics stage and body mass index of examined patients (11). However, the function of ATX was not investigated in preliminary studies.

An epidemiological study reported that endometrial carcinoma is frequently an estrogen-dependent tumor (12). The present study detected ATX expression in endometrial cancer cell lines. Ishikawa and Hec-1A endometrial cancer cell lines express high and low levels of ER, respectively. The mRNA and protein expression levels of ATX were higher in Ishikawa cells positive for ER and lower in Hec-1A cells with low ER expression. ATX expression was strongly positive in Ishikawa cells, with almost no expression in Hec-1A cells following immunohistochemistry staining. Hence, estrogen may participate in regulating ATX generation and secretion. The expression of ATX is regulated by a number of tumor microenvironment factors. Kehlen *et al* (13,14) demonstrated that epidermal growth factor and basic fibroblast growth factor promote ATX mRNA expression in thyroid cancer cells. The

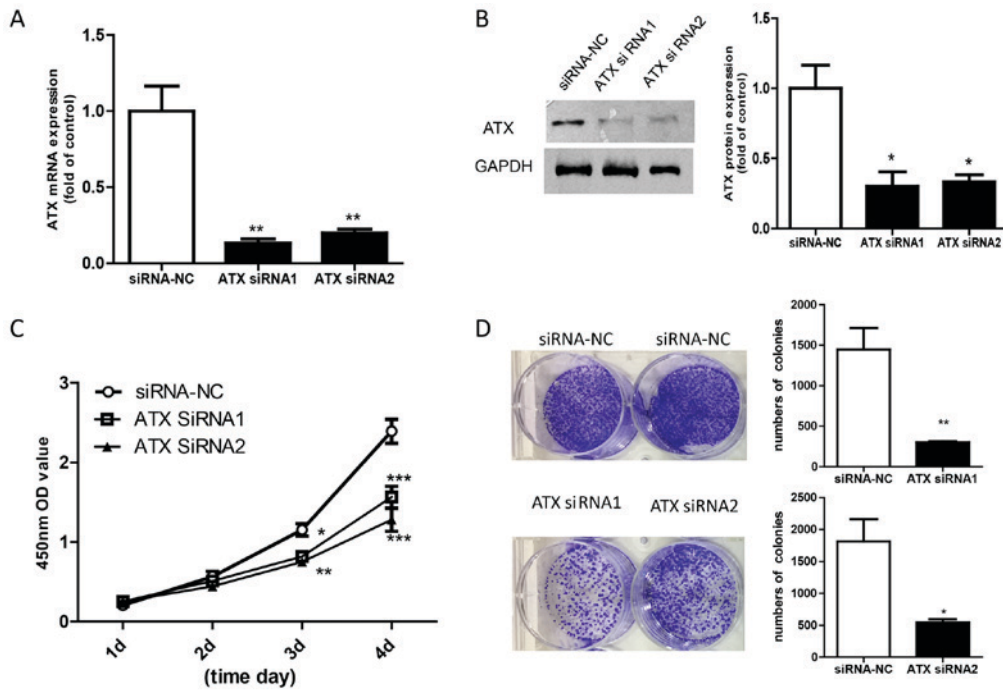


Figure 3. Knockdown of ATX with siRNA inhibited the proliferation of Ishikawa cells. (A) Ishikawa cells were transfected with siRNA-NC or siRNA1 and siRNA2 specific to the ATX gene for 48 h. The mRNA and protein expression of ATX were detected by reverse transcription-quantitative polymerase chain reaction and western blot analysis, respectively. The mRNA were detected by reverse transcription-quantitative polymerase chain reaction. (B) The protein expression of ATX was analyzed by western blot. Quantification of siRNA-NC, siRNA1 and siRNA2 groups. (C) Cell Counting kit-8 assay of cell proliferation of transfected cells at 1, 2, 3 and 4 days following siRNA knockdown of ATX. (D) Colony formation assay of proliferation of Ishikawa cells with siRNA knockdown of ATX. Data are shown as the mean ± standard deviation (n=3). *P<0.05, **P<0.01 and ***P<0.001 vs. siRNA-NC. siRNA-NC, nonsense negative control short interfering RNA; ATX, autotaxin; OD, optical density.

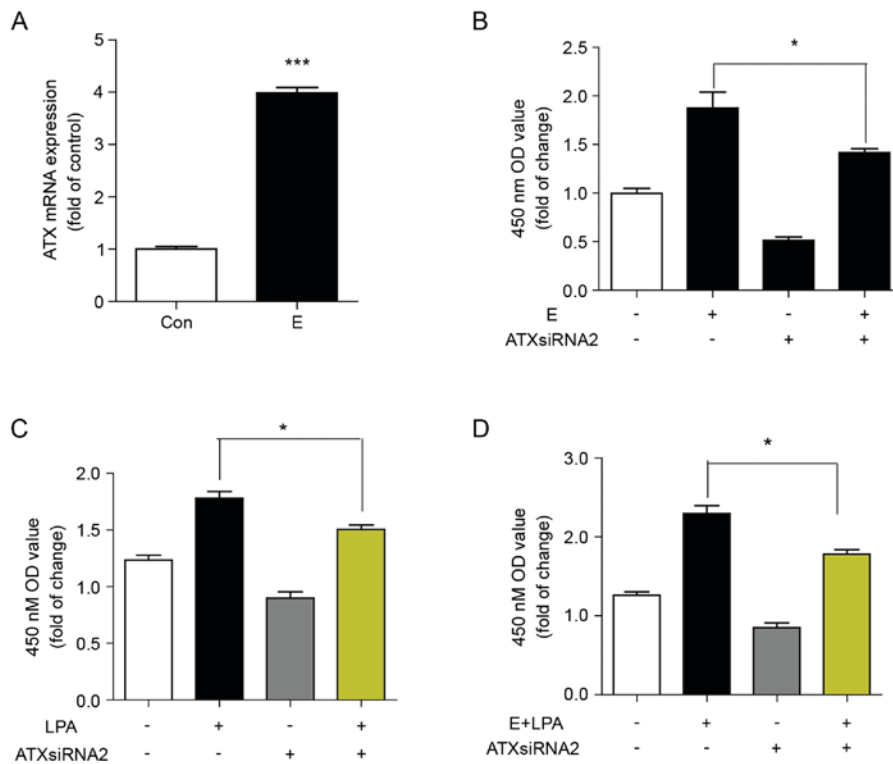


Figure 4. Reduced ATX levels protect against proliferation of Ishikawa cells induced by estrogen and LPA. (A) Reverse transcription-quantitative polymerase chain reaction of the mRNA expression of ATX in Ishikawa cells stimulated with 17β-estradiol (10 nM) for 24 h. ***P<0.001 vs. Con. (B) CCK8 assay of cell proliferation of Ishikawa cells transfected with ATX siRNA or siRNA-NC for 24 h, then 2,000 cells/pore were stimulated with or without 17β-estradiol for 48 h. *P<0.05, as indicated. (C) CCK8 assay of cell proliferation of Ishikawa cells transfected with ATX siRNA or siRNA-NC for 24 h, then stimulated with or without LPA for 48 h. *P<0.05, as indicated. (D) CCK8 assay of cell proliferation of Ishikawa cells transfected with ATX siRNA or siRNA-NC for 24 h, then stimulated with or without 17β-estradiol and LPA for 48 h. Data are shown as the mean ± standard deviation (n=3). *P<0.05, as indicated. E, 17β-estradiol; con, control; LPA, lysophosphatidic acid; ATX siRNA, autotaxin short interfering RNA; siRNA-NC, nonsense negative control short interfering RNA; OD, optical density; CCK, Cell Counting kit-8.

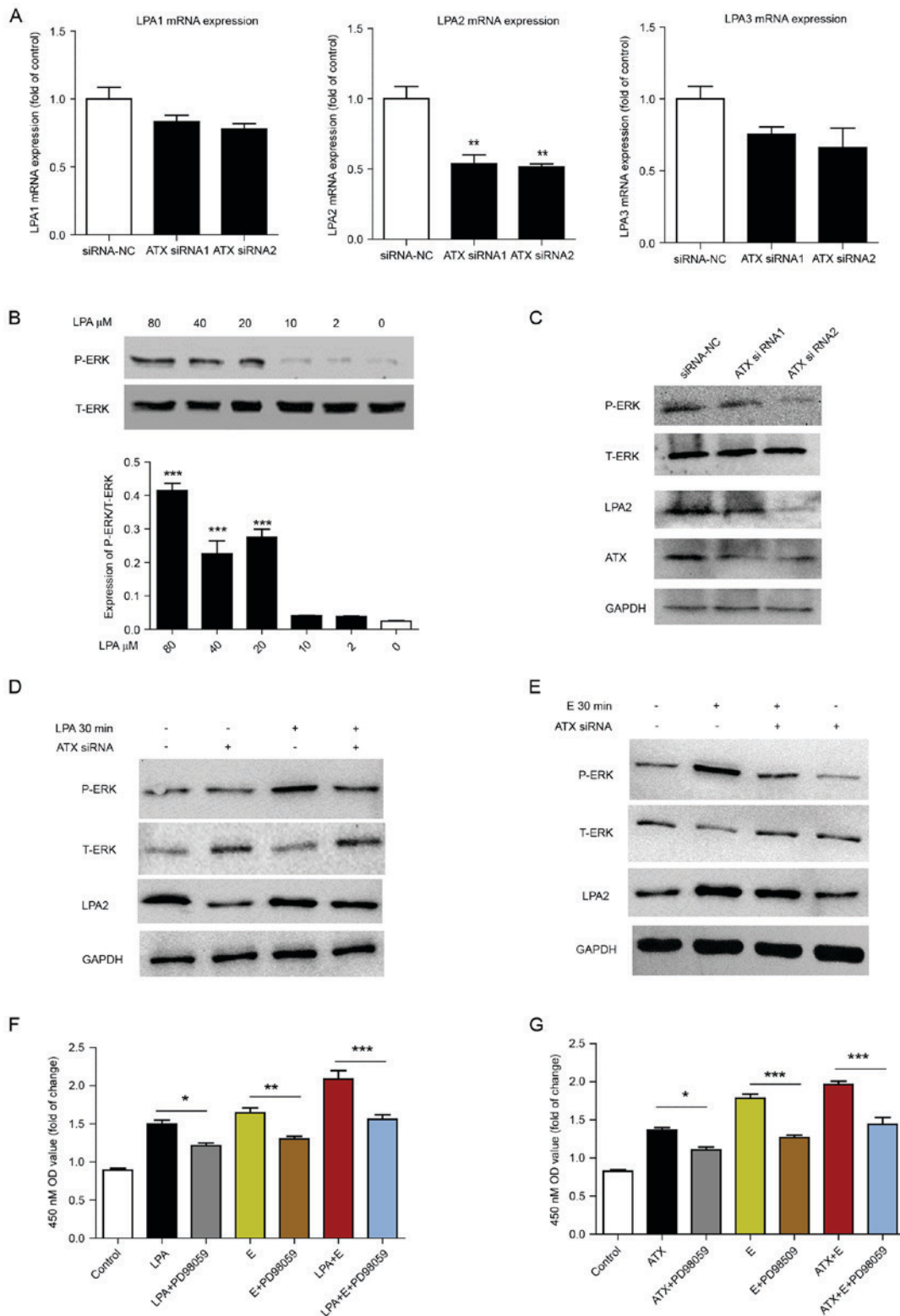


Figure 5. ATX-LPA axis is involved in estrogen-induced proliferation via ERK signaling. (A) Reverse transcription-quantitative polymerase chain reaction of the mRNA expression levels of LPA1, 2 and 3 in Ishikawa cells following siRNA knockdown of ATX for 24 h. ** $P < 0.01$ vs. siRNA-NC. (B) T-ERK and P-ERK levels following treatment with doses of LPA for 30 min in Ishikawa cells. *** $P < 0.001$ vs. 0 μ M LPA. Western blot analysis of the protein expression of ATX, LPA2, P-ERK and T-ERK in Ishikawa cells following (C) siRNA knockdown of ATX for 48 h, (D) combined treatment with or without 40 μ M LPA for 30 min, or (E) 17 β -estradiol (10 nM) for 30 min. Cell Counting kit-8 assay of cell proliferation following treatment with (F) LPA and/or 17 β -estradiol, plus 100 μ M PD98059 (ERK inhibitor) for 24 h and (G) 0.5 nM human recombinant ATX and/or 17 β -estradiol plus 100 μ M PD98059 for 24 h. Data are shown as the mean \pm standard deviation (n=3). * $P < 0.05$, ** $P < 0.01$ and *** $P < 0.001$, as indicated. ERK, extracellular signal-regulated kinase; T-ERK, total ERK; P-ERK, phosphorylated ERK; LPA, lysophosphatidic acid; ATX, autotaxin; OD, optical density; E, 17 β -estradiol.

present study confirmed that ATX mRNA levels were upregulated by estrogen. LPA receptor expression in Ishikawa and

Hec-A cells was examined, and the expression of LPA1, 2 and 3 was greater in the two cell types. This data suggested that

the ATX-LPA axis may serve a role in the development of endometrial carcinoma.

The results of cell proliferation in the present study demonstrated that with siRNA knockdown of ATX, cell colony number and cell proliferation rate decreased significantly. Sawada *et al* (15) revealed that concentrations of 1-15 $\mu\text{mol/l}$ LPA may stimulate the growth of ovarian cancer cells. Fishman *et al* (16) reported that LPA improved the expression of cell surface adhesion molecule-1 integrin in ovarian cancer cells and enhanced the ability of cell adhesion mediated by collagen I. Meng *et al* (17) demonstrated that LPA inhibited apoptosis induced by Fas and induced Fas translocation from the cell membrane to the cytoplasm. Therefore, LPA, as a biologically active substance with signal transduction, is closely associated with the growth, adhesion and metastasis of cancer cells (17). In the present study, it was revealed that ATX was involved in estrogen- and LPA-induced cell proliferation.

The results of the present study also showed that the mRNA expression levels of LPA2 decreased in Ishikawa cells transfected with ATX siRNA. ERK inhibitors may prevent the protective effect of LPA on cell apoptosis, which suggests that the Ras/Raf1/mitogen-activated protein kinase kinase/ERK signaling pathway may be involved in the protective effect of LPA on apoptosis (18). Therefore, in the current study, Ishikawa cells were treated with different concentrations of LPA to observe ERK phosphorylation. LPA induced ERK phosphorylation at high concentrations. In addition, ATX siRNA transfection reduced the estrogen- and LPA-induced ERK phosphorylation. The ERK inhibitor reduced the cell proliferation induced by estrogen, ATX and LPA. The results suggested that the mitogen-activated protein kinase (MAPK)/ERK signaling pathway may be involved in the estrogen-ATX-LPA axis, inducing the proliferation of endometrial cancer cells. The ATX-LPA axis may facilitate estrogen-induced proliferation of endometrial cancer via the MAPK/ERK signaling pathway.

The role of the ATX-LPA axis was preliminarily revealed in endometrial cancer. A recent study indicated that ATX may promote the recurrence and metastasis of breast cancer by regulating the tumor inflammation microenvironment (19). Whether the ATX-LPA axis is involved in regulating the imbalanced inflammatory microenvironment in endometrial carcinoma is unknown. Further investigation is required to study the role of the ATX-LPA axis in the progression of endometrial carcinoma. The present study will provide ideas and experimental basis for clinicians to identify novel molecular targeted drugs for the treatment of endometrial cancer.

Acknowledgements

The present study was funded by National Key Technology Research and Development Program of the Ministry of Science and Technology of China (grant no. 2015BAI13B06) and Research and Development Fund of Peking University People's Hospital (grant no. RD2014-06).

References

1. Globocan. 2012 <http://globocan.iarc.fr/Pages/online.aspx>. Accessed 4 July, 2016.

2. National Cancer Institute. PDQ® screening and prevention editorial board. PDQ endometrial cancer prevention. Bethesda, MD: National Cancer Institute. 2016; <http://www.cancer.gov/types/uterine/hp/endometrial-prevention-pdq>. (11 January 2015, date last accessed) [PMID: 26389477].
3. Jeppesen MM, Mogensen O, Hansen DG, Iachina M, Korsholm M and Jensen PT: Detection of recurrence in early stage endometrial cancer-the role of symptoms and routine follow-up. *Acta Oncol* 56: 262-269, 2017.
4. Busch EL, Crous-Bou M, Prescott J, Chen MM, Downing MJ, Rosner B, Mutter GL and De Vivo I: Endometrial cancer risk factors, hormone receptors, and mortality prediction. *Cancer Epidemiol Biomarkers Prev* 26: 727-735, 2017.
5. Benesch MG, Tang X, Venkatraman G, Bekele RT and Brindley DN: Recent advances in targeting the autotaxin-lysophosphatidate-lipid phosphate phosphatase axis in vivo. *J Biomed Res* 30: 272-284, 2016.
6. Volden PA, Skor MN, Johnson MB, Singh P, Patel FN, McClintock MK, Brady MJ and Conzen SD: Mammary adipose tissue-derived lysophospholipids promote estrogen receptor-negative mammary epithelial cell proliferation. *Cancer Prev Res (Phila)* 9: 367-378, 2016.
7. Gaetano CG, Samadi N, Tomsig JL, Macdonald TL, Lynch KR and Brindley DN: Inhibition of autotaxin production or activity blocks lysophosphatidylcholine-induced migration of human breast cancer and melanoma cells. *Mol Carcinog* 48: 801-809, 2009.
8. Ptaszynska MM, Pendrak ML, Bandle RW, Stracke ML and Roberts DD: Positive feedback between vascular endothelial growth factor-A and autotaxin in ovarian cancer cells. *Mol Cancer Res* 6: 352-363, 2008.
9. Hope JM, Wang FQ, Whyte JS, Ariztia EV, Abdalla W, Long K and Fishman DA: LPA receptor 2 mediates LPA-induced endometrial cancer invasion. *Gynecol Oncol* 112: 215-223, 2009.
10. Livak KJ and Schmittgen TD: Analysis of relative gene expression data using real time quantitative PCR and the 2(-Delta Delta C(T)) method. *Methods* 25: 402-408, 2001.
11. Wasniewski T, Woclawek-Potocka I, Boruszewska D, Kowalczyk-Zieba I, Sinderewicz E and Grycmacher K: The significance of the altered expression of lysophosphatidic acid receptors, utotaxin and phospholipase A2 as the potential biomarkers in type 1 endometrial cancer biology. *Oncol Rep* 34: 2760-2767, 2015.
12. Droog M, Nevedomskaya E, Dackus GM, Fles R, Kim Y, Hollema H, Mourits M, Nederlof PM, van Boven HH, Linn SC, *et al*: Estrogen receptor α wilds treatment-specific enhancers between morphologically similar endometrial tumors. *Proc Natl Acad Sci USA* 114: E1316-E1325, 2017.
13. Kehlen A, Englert N, Seifert A, Klonisch T, Dralle H, Langner J and Hoang-Vu C: Expression, regulation and function of autotaxin in thyroid carcinomas. *Int J Cancer* 109: 833-838, 2004.
14. Kehlen A, Lauterbach R, Santos AN, Thiele K, Kabisch U, Weber E, Riemann D and Langner J: IL-1 β - and IL-4-induced down-regulation of autotaxin mRNA and PC-1 in fibroblast-like synoviocytes of patients with rheumatoid arthritis(RA). *Clin Exp Immunol* 123: 147-154, 2001.
15. Sawada K, Morishige Ki, Tahara M, Ikebuchi Y, Kawagishi R, Tasaka K and Murata Y: Lysophosphatidic acid induces focal adhesion assembly through Rho/Rho-associated kinase pathway in human ovarian cancer cells. *Gynecol Oncol* 87: 252-259, 2002.
16. Fishman DA, Liu Y, Ellerbroek SM and Stack MS: Lysophosphatidic acid promotes matrix metalloproteinase (MMP) activation and MMP-dependent invasion in ovarian cancer cells. *Cancer Res* 61: 3194-3199, 2001.
17. Meng Y, Kang S and Fishman DA: Lysophosphatidic acid inhibits anti-Fas-mediated apoptosis enhanced by actin depolymerization in epithelial ovarian cancer. *FEBS Lett* 579: 1311-1319, 2005.
18. Sun H, Zhu Q, Ren J, Wu L, Kong FZ, Li G and Hu HF: Influence of lysophosphatidic acid on proliferation, adhesion, migration and apoptosis of cervical cancer HeLa cells. *Xi Bao Yu Fen Zi Mian Yi Xue Za Zhi* 25: 702-705, 2009 (In Chinese).
19. Benesch MG, Tang X, Dewald J, Dong WF, Mackey JR, Hemmings DG, McMullen TP and Brindley DN: Tumor-induced inflammation in mammary adipose tissue stimulates a vicious cycle of autotaxin expression and breast cancer progression. *FASEB J* 29: 3990-4000, 2015.



This work is licensed under a Creative Commons Attribution-NonCommercial-NoDerivatives 4.0 International (CC BY-NC-ND 4.0) License.